Available online www.jocpr.com

Journal of Chemical and Pharmaceutical Research, 2015, 7(12):891-897

Research Article

ISSN : 0975-7384
CODEN(USA) : JCPRC5

Density functional theory (DFT) and topological parameters based QSAR study of MK-886 analogues as bioactive mPGES-1 inhibitors

P. N. Tripathi*, Sunil Kumar Singh*[1] and Satish Kumar Singh[#]

**Department of Chemistry, KISAN (P.G.) College, Baharaich, U.P., India*
[#]Department of Chemistry, M. L. K. (P.G.) College, Balrampur, U.P., India

---

ABSTRACT

MK-886 derivatives are indole carboxylic acids. A series of MK-886 analogues showed selectivity and higher activity against the inducible mPGES-1 with the lowest IC_{50} value found being 3 nM. In this paper, DFT based quantum chemical and topological descriptors have been used for the development of QSAR models of MK-886 analogues. The descriptors that have been used are total energy, electron affinity, LogP, shape index (order 1), shape index (order 2), solvent accessibility surface area, valence connectivity index (order 1) and molar refractivity. Evaluation of descriptors has been done with the help of CAChe Pro software, using the DFT and PM3 Methods. The Project Leader program has been used for multi linear regression (MLR) analysis. Reliable QSAR models have been obtained from single descriptors namely total energy, LogP, shape index (order 2) and solvent accessibility surface area, therefore these descriptors appear important for the study of MK-886 analogues. It has been observed from our study that the best combination of descriptors is total energy, shape index (order 1), solvent accessibility surface area and valence connectivity index (order 1) for the QSAR study of MK-886 analogues and can be used to find out the activity of any new derivative of MK-886.

Keywords: MK-886 analogues, DFT, quantum chemical descriptors, topological descriptors.

INTRODUCTION

The prostaglandins are a group of hormone like lipid compounds that are derived enzymatically from fatty acids and have important functions in the animal body. Every prostaglandin contains 20 carbon atoms, including a 5-carbon ring. They are mediators and have a variety of strong physiological effects, such as regulating the contraction and relaxation of smooth muscle tissue [1]. Prostaglandins are potent but have a short half-life before being inactivated and excreted. Therefore, they send only paracrine (locally active) or autocrine (acting on the same cell from which it is synthesized) signals. Prostaglandin E synthase (or PGE synthase) is an enzyme involved in eicosanoid and glutathione metabolism, a member of MAPEG family. It generates prostaglandin E (PGE) from prostaglandin H2 [2, 3]. There are three forms of prostaglandin E synthase (PGES), namely, microsomal prostaglandin E2 synthase-1 (mPGES-1), microsomal prostaglandin E2 synthase-2 (mPGES-2) and cytosolic PGES. The pathway linkage preference of mPGES-1, mPGES-2 and cPGES is, both COX-1 and COX-2 respectively [4]. The mPGES-1 is an important enzyme because it catalyses the conversion of prostaglandin endoperoxide (PG) H2 to PGE2. PGE2 in turn controls biological activities such as relaxation and contraction of muscles. Microsomal prostaglandin E synthase-1 is a member of the membrane associated proteins involved in eicosanoid and glutathione metabolism (MAPEG) superfamily [5].

There are several examples of compounds that were identified and developed to target mPGES-1 [6, 7]. MK-886 derivatives are actually indole carboxylic acids. Compound MK-886 is (3-[3-(4-chlorobenzyl)-3-t-butyl-thio-5-isopropylindol-2-yl] 2, 2-di-methylpropanoic acid). A series of MK-886 compounds also showed selectivity and higher activity against the inducible mPGES-1 with the lowest IC_{50} value found being 3 nM. [8].

In this paper, quantum chemical and topological descriptors have been used for the development of QSAR models of MK-886 analogues. The descriptors that have been used are total energy, electron affinity, LogP, shape index (order 1), shape index (order 2), solvent accessibility surface area, valence connectivity index (order 1) and molar refractivity.

EXPERIMENTAL SECTION

The study material of this paper is thirty Indole analogues of MK-886 compound (as inhibitors of mPGES-1) given in Table-1. Their observed biological activities are in terms of IC_{50} values. The IC_{50} values, *i.e.*, the concentration (μM) of inhibitor that produces 50% inhibition of mPGES-1 were converted into pIC_{50} ($-\log IC_{50}$) as reported in Table 1. The 3D modeling and geometry optimization of all the compounds and evaluation of values of descriptors have been done with the help of CAChe Pro software of Fujitsu, using the DFT Methods [9-16] and semiemperical PM3 Hamiltonian [17]. The Project Leader program has been used for multi linear regression (MLR) analysis. The statistical parameters have been calculated by Smith's Statistical Package (version 2.80).

The descriptors that have been evaluated are discussed below,

Water/Octanol Partition coefficient (Log P): [18]
The Water/Octanol partition coefficient is the ratio of concentrations of un-ionized compound between the two solutions. To measure the partition coefficient of ionizable solutes, the pH of the aqueous phase is adjusted such that the predominant form of the compound is un-ionized. The logarithm of the ratio of the concentrations of the un-ionized solute in the solvents is called log P

$$log\ P_{oct/wat} = log\left(\frac{[solute]_{octanol}}{[solute]_{water}^{un-ionized}}\right)$$

Molar Refractivity: [19]
It is a constitutive-additive property that is calculated by the Lorenz-Lorentz formula,

$$MR = \frac{n^2-1}{n^2+2} * \frac{M}{p}$$

where M is the molecular weight, n is the refraction index and ρ is the density. For a radiation of infinite wavelength, the molar refractivity represents the real volume of the molecules.

Total energy:
Total energy (TE) of a molecular system is sum of the total electronic energy (Eee) and the energy of internuclear repulsion (Enr) [20].

TE = Eee + Enr

The total electronic energy of the system is given by

Eee =1 /2 P (H +F)

Where P is the density matrix, H is the one-electron matrix, and F is the Fock matrix.

Electron Affinity [21]:
Parr et al define the electronegativity as the negative of chemical potential [22] as

$\chi = -\mu$ = 1 / 2 (IP+EA)

where IP and EA are the ionization potential and electron affinity respectively, of the chemical species. According to the Koopman's theorem, the IP is simply the eigen value of HOMO with change of sign and EA is the eigen value of LUMO with change of sign, hence we have

EA = ε HOMO

The energy gained when an electron is added to the lowest unoccupied molecular orbital (LUMO) is the eigen value of LUMO.

Solvent Accessibility Surface Area (SASA):
It is the surface area of a biomolecule that is accessible to a solvent and is usually quoted in square angstrom. Lee and Richards first described the solvent accessible surface area (SASA) of a molecular surface. SASA is typically calculated by using the 'rolling ball' algorithm developed by Sharke & Rupley.

Valence connectivity index (χ):
This index, originally defined by Randic and subsequently refined by Kier and Hall, is a series of numbers designated by "order" and "subgraph type"[23, 24]. There are four subgraph types; path, cluster, path/cluster, and chain. These types emphasize different aspects of atom connectivity within a molecule, the amount of branching, ring structures present and flexibility. It is calculated from the hydrogen suppressed molecular graph and defined as follows,

$$^{m}\chi^{v} = \sum_{i=1}^{N_S} \prod_{k=1}^{m+1} \left[\frac{1}{\delta_k^v} \right]^{1/2}$$

Where, $\delta_k^v = \frac{(Z_k^v - H_k)}{(Z_k - Z_k^v - 1)}$ - valence connectivity for the k-th atom in the molecular graph, Z_k = the total number of electrons in the k-th atom, Z^v_k = the number of valence electrons in the k-th atom, H_k = the number of hydrogen atoms directly attached to the kth non-hydrogen atom, m = 0 - atomic valence connectivity indices (called order-0), m = 1 - one bond path valence connectivity indices (called order-1), m = 2 - two bond fragment valence connectivity indices (called order-2).

Shape indices (κ_n):
These indices compare the molecule graph with "minimal" and "maximal" graphs, where the meaning of "minimal" and "maximal" depends on the order "n". This is intended to capture different aspects of the molecular shape. Kier was first to propose shape indices for molecular graphs, the so called kappa shape indices [25, 26]. The first order kappa shape index (1κ or κ_1) is given by,

$$^{1}K = \frac{A(A-1)^2}{(^{1}P)^2}$$

Where, iP = Length of paths of bond length i in the hydrogen suppressed molecule and A is the number of non-hydrogen atoms in the molecule.

The second order kappa shape index (2κ or κ_2) is given by

$$^{2}K = \frac{(A-1)(A-2)^2}{(^{2}P)^2}$$

The third order kappa shape index (3κ or κ_3) is given by

$$^{3}K = \frac{(A-1)(A-3)^2}{(^{3}P)^2} \qquad \text{if "A" is odd}$$

$$^{3}K = \frac{(A-3)(A-2)^2}{(^{3}P)^2} \qquad \text{if "A" is even}$$

RESULTS AND DISCUSSION

Thirty compounds given in Table-1 have been considered. The values of eight descriptors of compounds have been calculated and presented in Table-2 along with their observed biological activities in terms of IC_{50} values. The IC_{50}

values were converted into pIC_{50}(-logIC_{50}). QSAR models using different combinations of descriptors have been examined. Four QSAR models with good predictive power have been obtained from single descriptors namely total energy, LogP, shape index (order 2) and solvent accessibility surface area. The MLR equations for these four models are given below,

$^{Mono-}$PA1 = -0.0266117*E_T - 5.79315.
r^2 = 0.717996, rCV^2 = 0.653989, Std. Error = 0.1184, SEE = 0.6358,
t-value = 8.4440, p-value = 0, DOF = 0.7080, N = 30.

$^{Mono-}$PA2 = 0.508528*SI(2) - 4.98673.
r^2 = 0.69226, rCV^2 = 0.624623, Std. Error = 0.1260, SEE = 0.6641,
t-value = 7.9374, p-value = 0, DOF = 0.6813, N = 30.

$^{Mono-}$PA3 = 0.643887*LogP - 4.5632.
r^2 = 0.672017, rCV^2 = 0.623559, Std. Error = 0.1320, SEE = 0.6857,
t-value = 7.5740, p-value = 0, DOF = 0.6603, N = 30.

$^{Mono-}$PA4 = 0.0146111*SASA - 6.26992.
r^2 = 0.657249, rCV^2 = 0.573832, Std. Error = 0.1365, SEE = 0.7009,
t-value = 7.3276, p-value = 0, DOF = 0.6450, N = 30.

In the above regression equations, r^2 is correlation coefficient, rCV^2 is cross-validation coefficient, Std. Error is standard error, SEE is standard error of estimate, DOF is degrees of freedom and N is data points (compounds). From the above MLR equations, it is clear that total energy, LogP, shape index (order 2) and solvent accessibility surface area appear as good descriptors for MK-886 analogues.

The addition of other descriptors in the above mono-parametric models yield the QSAR models with improved predictability. The resulting bi-parametric QSAR model obtained by using descriptors total energy and valence connectivity index (order 1) is given by following regression equation,

$^{Bi-}$PA1 = -0.057396*E_T - 0.702476*VCI(1) - 4.72495.
r^2 = 0.843675, rCV^2 = 0.825247, Std. Error = 0.0813, SEE = 0.4734,
t-value = 12.2923, p-value = 0, DOF = 0.8381, N = 30.

and the bi-parametric QSAR model developed from descriptors solvent accessibility surface area and valence connectivity index (order 1) is given by following regression equation,

$^{Bi-}$PA2 = 0.0431476*SASA - 1.10391*VCI(1) - 6.3799.
r^2 = 0.833195, rCV^2 = 0.802865 Std. Error = 0.0846, SEE = 0.4891,
t-value = 11.8233, p-value = 0, DOF = 0.8272, N = 30.

Using combination of three descriptors, the tri-parametric QSAR models are obtained with improved predictive power. The best two are discussed here,

$^{Tri-}$PA1 = -0.0335434*E_T + 0.022387*SASA - 1.03036*VCI(1) -5.56509.
r^2 = 0.878134, rCV^2 = 0.859215, Std. Error = 0.0704, SEE = 0.4180,
t-value = 14.2028, p-value = 0, DOF = 0.8738, N = 30.

This QSAR model involves total energy as first descriptor, solvent accessibility surface area as second descriptor and valence connectivity index (order 1) as third descriptor.

$^{Tri-}$PA2 = -0.0479737*E_T + 0.286908*LogP - 0.715643*VCI(1) - 4.5997.
r^2 = 0.875686, rCV^2 = 0.81368, Std. Error = 0.0712, SEE = 0.4220,
t-value = 14.0478, p-value = 0, DOF = 0.8713, N = 30.

This QSAR model involves total energy as first descriptor, LogP as second descriptor and valence connectivity index (order 1) as third descriptor. From the values of correlation coefficient (r^2), cross-validation coefficient (rCV^2) and other statistical parameters for the above two QSAR models, it is clear that the predictive power of models is high and can be used to find out the activity of any new derivative of MK-886.

By the combination of four descriptors, tetra-parametric QSAR models are obtained with excellent predictive power. The best tetra-parametric QSAR model is obtained by following regression equation,

$^{Tetra-}$PA1 = -0.0550818*E_T - 0.38797*SI(1) + 0.0298816*SASA
- 0.91611*VCI(1) - 5.15002.
r^2 = 0.910763, rCV^2 = 0.886327, Std. Error = 0.0591, SEE = 0.3576,
t-value = 16.9057, p-value = 0, DOF = 0.9076, N = 30.

The above QSAR model is obtained by using the descriptors total energy, shape index (order 1), solvent accessibility surface area and valence connectivity index (order 1). From the values of correlation coefficient (r^2), cross-validation coefficient (rCV^2) and other statistical parameters for the above QSAR model, it is clear that the predictive power of this model is excellent and can be used to find out the activity of any new derivative of MK-886. The predicted pIC_{50} values obtained from above mono-, bi-, tri- and tetra-parametric QSAR models are listed in Table-3 alongwith their observed pIC_{50} values.

Table-1: Thirty Indole derivatives of MK-886 compounds used in our study

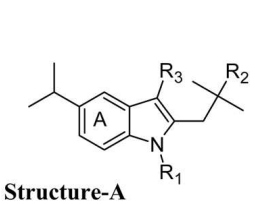

Structure-A

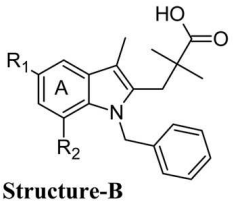

Structure-B

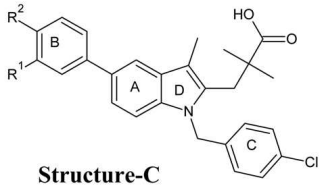

Structure-C

S.No.	Structure	R1	R2	R3	IC50	pIC50
1	A	CH2(4-Cl-Ph)	COOH	S-tertBu	1.6	-0.204
2	A	H	COOH	S-tertBu	10	-1.041
3	A	Me	COOH	S-tertBu	10	-1.041
4	A	CH2(CH=CH2)	COOH	S-tertBu	6.7	-0.826
5	A	(CH2)3Ph	COOH	S-tertBu	3.2	-0.50
6	A	CH2(4-Cl-Ph)	COOMe	S-tertBu	7.2	-0.857
7	A	CH2(4-Cl-Ph)	$COONH_2$	S-tertBu	10	-1.041
8	A	CH2(4-Cl-Ph)	COOH	OPh	0.65	0.187
9	A	CH2(4-Cl-Ph)	COOH	CH2(4-tertBu-Ph)	0.29	0.538
10	A	CH2(4-Cl-Ph)	COOH	CO(2-Me-Ph)	0.9	0.046
11	A	CH2(4-Cl-Ph)	COOH	COCH2S-tertBu	0.26	0.585
12	A	CH2(4-Cl-Ph)	COOH	COCH2-tertBu	0.25	0.602
13	A	CH2(4-Cl-Ph)	COOH	Me	1.1	-0.041
14	B	H	iso-propyl		4.3	-0.633
15	B	H	H		3.2	-0.505
16	B	F	H		2.6	-0.415
17	B	tert-butyl	H		0.33	-0.481
18	B	Ph	H		0.6	0.222
19	C	Ph	H		0.16	0.796
20	C	H	Ph		0.016	1.796
21	C	Cl	Ph		0.022	1.658
22	C	F	Ph		0.007	2.155
23	C	F	1,3-pyrazinyl		0.032	1.495
24	C	F	3-pyridinyl		0.012	1.921
25	C	F	2-MeO-Ph		0.005	2.301
26	C	F	2-Cl-Ph		0.004	2.398
27	C	F	2-F-Ph		0.008	2.097
28	C	F	2-MeCO-Ph		0.006	2.222
29	C	F	3-Me-Ph		0.033	1.481
30	C	F	4-Me-Ph		0.031	1.509

Table-2: Values of descriptors and observed activities of MK-886 analogues

C. No.	E_T	EA	LogP	SI (1)	SI (2)	SASA	VCI (1)	MR	pIC50
1	-230.966	0.358	7.682	26.602	10.318	451.936	12.296	136.317	-0.204
2	-175.931	0.051	5.14	20.314	7.319	360.08	9.291	102.003	-1.041
3	-183.036	0.133	5.387	21.302	7.553	378.713	9.685	106.9	-1.041
4	-195.514	0.052	6.128	23.281	8.789	407.308	10.371	116.063	-0.826
5	-233.53	0.287	7.812	27.585	11.373	480.053	12.819	140.868	-0.5
6	-238.114	0.31	7.713	27.585	10.948	464.413	12.685	141.087	-0.857
7	-228.185	0.313	6.817	26.602	10.318	461.479	12.361	138.14	-1.041
8	-241.504	0.305	8.186	27.046	11.588	467.133	11.89	135.848	0.187
9	-265.431	0.266	8.781	28.135	9.25	517.33	14.677	150.436	0.538
10	-253.973	0.281	8.446	28.994	12.027	476.11	12.603	145.224	0.046
11	-255.557	0.414	7.065	29.554	11.807	506.175	13.358	146.442	0.585
12	-246.404	0.413	7.854	28.569	11.171	477.548	12.233	138.262	0.602
13	-200.305	0.27	7.224	22.68	9.013	408.85	10.072	114.648	-0.041
14	-188.497	0.031	6.706	21.703	8.789	358.081	9.6	109.844	-0.633
15	-167.027	0.056	5.512	18.781	7.709	335.946	8.24	95.653	-0.505
16	-182.862	0.178	5.652	19.753	7.935	343.92	8.34	95.869	-0.415
17	-195.701	0.009	7.14	22.68	8.626	399.364	9.901	114.319	-0.481
18	-203.237	0.096	7.197	23.168	9.868	413.65	10.311	120.789	0.222
19	-251.212	0.334	9.399	28.526	12.25	511.348	12.86	150.73	0.796
20	-251.22	0.304	9.399	28.526	12.25	509.2	12.86	150.73	1.796
21	-262.988	0.368	9.917	29.491	12.475	523.732	13.344	155.535	1.658
22	-267.136	0.452	9.539	29.491	12.475	515.753	12.966	150.946	2.155
23	-271.429	0.724	7.314	29.491	12.475	508.723	12.675	146.261	1.495
24	-269.287	0.624	8.227	29.491	12.475	512.023	12.816	148.789	1.921
25	-286.507	0.298	9.286	31.426	13.329	541.488	13.495	157.409	2.301
26	-278.899	0.474	10.057	30.458	12.701	528.7	13.449	155.751	2.398
27	-283.043	0.512	9.678	30.458	12.701	522.94	13.072	151.163	2.097
28	-291.789	0.501	8.847	32.395	13.553	547.996	13.837	161.349	2.222
29	-274.322	0.413	10.006	30.458	12.701	533.361	13.377	155.987	1.481
30	-274.321	0.423	10.006	30.458	12.701	534.369	13.377	155.987	1.509

where E_T = Total Energy, EA = Electron Affinity, LogP = LogP, SI (1)= Shape Index (order 1), SI (2)= Shape Index (order 2), SASA = Solvent Accessibility Surface Area, VCI (1) = Valence Connectivity Index (order 1), MR = Molar Refractivity.

Table-3: Predicted activities PA10 to PA18 of the 30 MK-886 analogues

C. No.	pIC50	$^{Mono-}$PA1	$^{Mono-}$PA2	$^{Mono-}$PA3	$^{Mono-}$PA4	$^{Bi-}$PA1	$^{Bi-}$PA2	$^{Tri-}$PA1	$^{Tri-}$PA2	$^{Tetra-}$PA1
1	-0.204	0.353	0.26	0.383	0.333	-0.106	-0.454	-0.37	-0.115	-0.509
2	-1.041	-1.111	-1.265	-1.253	-1.009	-1.154	-1.1	-1.176	-1.334	-1.092
3	-1.041	-0.922	-1.146	-1.095	-0.737	-1.023	-0.731	-0.927	-1.205	-0.889
4	-0.826	-0.59	-0.518	-0.618	-0.319	-0.789	-0.254	-0.574	-0.884	-0.743
5	-0.5	0.421	0.797	0.467	0.744	-0.326	0.183	-0.193	-0.329	-0.388
6	-0.857	0.543	0.58	0.403	0.516	0.031	-0.345	-0.251	-0.041	-0.48
7	-1.041	0.279	0.26	-0.174	0.473	-0.312	-0.114	-0.317	-0.543	-0.437
8	0.187	0.634	0.906	0.708	0.555	0.784	0.65	0.742	0.825	0.725
9	0.538	1.27	-0.283	1.091	1.289	0.199	-0.261	-0.203	0.15	0.567
10	0.046	0.966	1.13	0.875	0.687	0.999	0.251	0.627	0.988	0.272
11	0.585	1.008	1.017	-0.014	1.126	0.56	0.715	0.576	0.128	0.349
12	0.602	0.764	0.694	0.494	0.708	0.824	0.721	0.787	0.72	0.402
13	-0.041	-0.463	-0.403	0.088	-0.296	-0.303	0.143	-0.071	-0.125	0.074
14	-0.633	-0.777	-0.518	-0.245	-1.038	-0.65	-1.527	-1.117	-0.503	-1.282
15	-0.505	-1.348	-1.066	-1.014	-1.361	-0.927	-0.981	-0.932	-0.902	-0.746
16	-0.415	-0.927	-0.952	-0.924	-1.245	-0.088	-0.747	-0.325	-0.174	-0.104
17	-0.481	-0.585	-0.6	0.034	-0.435	-0.447	-0.078	-0.261	-0.248	-0.306
18	0.222	-0.385	0.031	0.071	-0.226	-0.303	0.085	-0.112	-0.164	-0.03
19	0.796	0.892	1.243	1.489	1.201	0.66	1.487	1.058	0.945	1.119
20	1.796	0.892	1.243	1.489	1.17	0.66	1.394	1.01	0.946	1.055
21	1.658	1.205	1.357	1.822	1.382	0.996	1.488	1.232	1.313	1.32
22	2.155	1.316	1.357	1.579	1.266	1.499	1.56	1.582	1.674	1.656
23	1.495	1.43	1.357	0.146	1.163	1.95	1.578	1.868	1.449	1.949
24	1.921	1.373	1.357	0.734	1.211	1.728	1.565	1.726	1.508	1.801
25	2.301	1.831	1.792	1.416	1.642	2.24	2.087	2.263	2.152	2.257
26	2.398	1.629	1.472	1.912	1.455	1.835	1.585	1.768	2.04	1.873
27	2.097	1.739	1.472	1.668	1.371	2.338	1.754	2.168	2.401	2.275
28	2.222	1.972	1.905	1.133	1.737	2.303	1.99	2.234	2.035	2.053
29	1.481	1.507	1.472	1.879	1.523	1.623	1.867	1.794	1.858	1.827
30	1.509	1.507	1.472	1.879	1.538	1.623	1.91	1.817	1.858	1.857

Figure-1: Trend of observed activity (pIC50) and predicted activity (obtained from $^{Tetra-}$PA1) of 30 MK-886 analogues

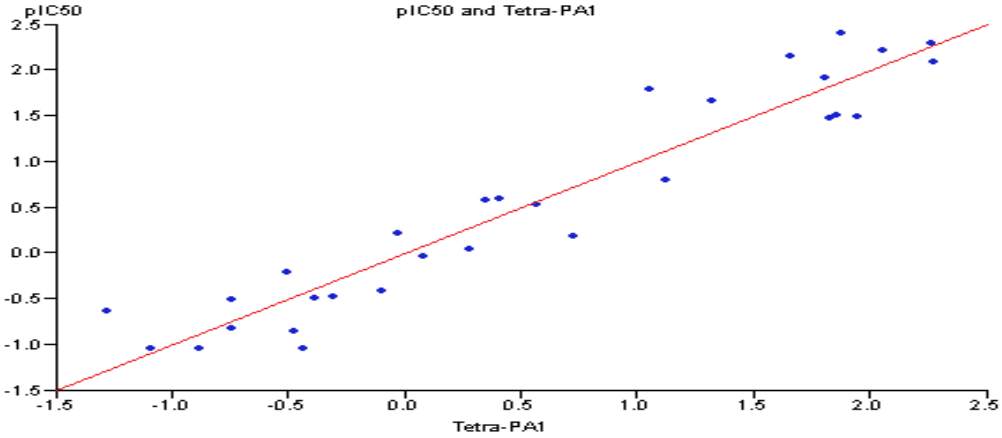

CONCLUSION

It is clear from above study that the best combination of descriptors is total energy, shape index (order 1), solvent accessibility surface area and valence connectivity index (order 1) for the QSAR study of MK-886 analogues and can be used to find out the activity of any new derivative of MK-886. The trend of observed activity and predicted activity obtained from $^{Tetra-}$PA1 is shown in figure-1. Reliable QSAR models have been obtained from single descriptors namely total energy, LogP, shape index (order 2) and solvent accessibility surface area, therefore these descriptors appear important for the study of MK-886 analogues.

REFERENCES

[1] Nelson, F Randy, An introduction to behavioural endocrinology, 3rd Edition, Sinauer Associates, **2005**, 100. ISBN 0-87893-617-3.
[2] C Jegerschold, SC Pawelzik, P Purhonen, P Bhakat, KR Gheorghe, N Gyobu, K Mitsuoka, R Morgenstern, PJ Jakobsson, H Hebert, *Proceedings of the National Academy of Sciences*, **2008,** 105 (32), 11110.
[3] M Murakami, Y Nakatani, T Tanioka, I Kudo, *Prostaglandins & Other Lipid Mediators*, **2002**, 68-69, 383.
[4] M Murakami, I Kudo, *Progress in Lipid Research*, **2004**, 43, 3-35.
[5] BP van Rees, A Sivula, S Thoren, *Int. J. Cancer*., **2003**, 107(4), 551.
[6] S Thoren, PJ Jakobsson, *Eur. J. Biochem.*, **2000**, 267, 6428.
[7] O Quraishi, JA Mancini, D Riendeau, *Biochem Pharmacol.*, **2002**, 63, 1183.
[8] D Riendeau, R Aspiotis, D Ethier, Y Gareau, EL Grimm, J Guay, S Guiral, H Juteau, JA Mancini, N Methot, J Rubin, RW Friesen, *Bioorg. Med. Chem. Lett.*, **2005**, 15, 3352.
[9] RG Parr, W Yang, Density-Functional Theory of Atoms and Molecules, Oxford University Press, New York, **1989**.
[10] RM Dreizler, EKU Gross, Density Functional Theory, Springer, Berlin, **1990**.
[11] JP Perdew, S Kurth, A Primer in Density Functional Theory, Springer, Berlin, **2003**.
[12] W Koch, MC Holthausen, A Chemist's Guide to Density Functional Theory, Wiley-VCH, New York **2000**.
[13] RG Pearson, Chemical Hardness: Applications from Molecules to Solids, Wiley-VCH, Oxford **1997**.
[14] H Chermette, *J. Comput. Chem.* **1999**, 20, 129-154.
[15] P Geerlings, F De Proft, W Langenaeker, *Chem. Rev.*, **2003**, 103, 1793-1873.
[16] PK Chattaraj, U Sarkar, DR Roy, *Chem. Rev.*, **2006**, 106, 2065-2091.
[17] RC Bingham, MJS Dewar, DH Lo, *J. Am. Chem. Soc*., **1975**, 97, 1285.
[18] P Pulay, W Sawodny, *Mol Phys*., **1975**, 30, 1123.
[19] RJ Padron, A Carrasco, RF Pellon, *Pharmaceutical Chemistry Centre.*, **2002**, 5, 258.
[20] RG Parr, W Young, *Annu. Rev. Phys. Chem.*, **1995**, 46, 701.
[21] T Saartok, E Dahlberg, JA Gustafsson, *Endocrinology*, **1984**, 114, 2100.
[22] T Saartok, E Dahlberg, JA Gustafsson, *Endocrinology*, **1984**, 114, 2100.
[23] AT Balaban, *Jour. of. Mol. Struc: THEOCHEM*, **1985**, 120, 117-142.
[24] M Petitjean, *J. Chem. Inf. Comput. Sci*., **1992**, 32, 331-337**.**
[25] LB Kier, *Quant. Struct.-Act. Relat.*, **1986**, 5, 1-7.
[26] L. B Kier, *Med. Res. Rev.*, **1987**, 7, 417-440.